Visualization of the Development of Multicellular Structures

F. David Fracchia
Przemyslaw Prusinkiewicz
Department of Computer Science
University of Regina
Regina, Saskatchewan, Canada S4S 0A2

Martin J. M. de Boer
Theoretical Biology Group
University of Utrecht
Padualaan 8, 3584 CH Utrecht, The Netherlands

Abstract

This paper presents a simulation-based method for visualizing the development of multicellular structures in two and three dimensions. The neighborhood relations between the cells are determined by a simulated developmental process, expressed using the formalism of map L-systems and its extension, cellwork L-systems. The cell shapes result from mechanical cell interactions. Two types of forces are considered: the osmotic pressure within cells, and the tension of cell walls. The method is illustrated using examples based on biological data.

Keywords: mathematical modeling in biology, simulation, visualization of development, map L-system, cellwork, dynamic model.

1 Introduction

An important issue in biology is the study of cell division patterns, that is, the spatial and temporal organization of cell divisions in tissues. This paper presents a method for simulating and visualizing the developmental processes.

On a *topological* level, cell divisions are expressed using the formalism of *map L-systems* operating on a plane or a sphere, or *cellwork L-systems* describing fully three-dimensional structures. Cell *geometry* is determined by a dynamic method that takes into account the osmotic pressure inside the cells and the tension of cell walls. The development can be animated by considering periods of continuous cell expansion, delimited by instantaneous cell divisions.

For two-dimensional structures, a modeling method using map L-systems with dynamic interpretation has been previously reported in [5]. The reader is referred to that paper for the biological motivation and a technique for constructing map L-systems capturing observed developmental patterns. A further biological discussion of the models is included in [3].

This paper is organized as follows. Section 2 reviews the method for simulating the development of planar cellular layers. Two models of fern gametophytes and a model of a moss leaf are used as examples. Section 3 extends this method to the surface of a sphere, and applies it to simulate the development of a snail embryo. Section 4 presents a further extension to three-dimensional cellular structures. Marker-based cellwork L-systems are proposed to describe structure topology and the dynamic interpretation rules are modified to operate in three dimensions. The formalism is applied to model the development of epidermal cells. Section 5 discusses open problems.

2 Modeling Planar Cell Layers

2.1 Maps

From a mathematical perspective, cellular layers can be represented using a class of planar graphs with cycles, called *maps* [12]. Nakamura *et al.* [10] characterize them as follows:

- A map is a finite set of *regions*. Each region is surrounded by a boundary consisting of a finite, circular sequence of *edges* which meet at *vertices*.
- Each edge has one or two vertices associated with it.[1] The edges cannot cross without forming a vertex and there are no vertices without an associated edge.
- Every edge is a part of the boundary of a region.
- The set of edges is connected. Specifically, there are no islands within regions.

Regions represent cells, and edges represent cell walls perpendicular to the plane of view. The internal components of a cell are not considered.

[1] The one-vertex case occurs when an edge forms a loop.

2.2 mBPM0L-systems

The process of cell division can be expressed as map rewriting. This notion is an extension of string rewriting found in formal language theory. Several map-rewriting systems have been described in the past [3]. We have chosen *Binary Propagating Map 0L-system with markers*, or mBPM0L-systems, proposed by Nakamura, Lindenmayer and Aizawa [10] as a refinement of the basic concept of map L-systems introduced by Lindenmayer and Rozenberg [8]. The name is derived as follows. A *map 0L-system* is a parallel rewriting system which operates on maps and modifies regions irrespective of what happens to other neighboring regions (a *context-free* mechanism). The system is *binary* in that a region can split into at most two daughter regions. It is *propagating* in the sense that edges cannot be erased, thus regions (cells) cannot fuse or die. The *markers* represent a technique for specifying the positions of inserted edges that split the regions.

Formally, an mBPM0L-system $\mathcal{G}$ consists of a finite alphabet of *edge labels* Σ, a *starting map* ω with labels from Σ, and a finite set of *edge productions* P. In general, the edges are *directed*, which is indicated by a left or right arrow placed above the edge symbol. In some cases, the edge direction has no effect on the system's operation. Such an edge is called *neutral* and no arrow is placed above the symbol denoting it. Each production is of the form $\mathtt{A} \rightarrow \alpha$. The directed or neutral edge $\mathtt{A} \in \Sigma$ is called the *predecessor*. The string α, composed of symbols from Σ and special symbols [,], + and −, is called the *successor*. The sequence of symbols outside the square brackets specifies the edge subdivision pattern. Arrows can be placed above edge symbols to indicate whether the successor edges have directions consistent with, or opposite to, the predecessor edge. Pairs of matching brackets [and] delimit *markers*, which specify possible attachment sites for region-dividing walls. The markers are viewed as short branches which can be interconnected to form a complete wall. The strings inside brackets consist of two symbols. The first symbol is either + or −, indicating whether the marker should be placed to the left or to the right of the predecessor edge. The second symbol is the marker label, with or without an arrow. The left arrow indicates that the marker is directed towards the predecessor edge, and the right arrow indicates that the marker is oriented away from that edge. If no arrow is present, the marker is neutral.

For example, in the production $\vec{\mathtt{A}} \rightarrow \vec{\mathtt{D}}\,\overleftarrow{\mathtt{C}}\,[-\,\overleftarrow{\mathtt{E}}]\,\vec{\mathtt{B}}\,\mathtt{F}$, the directed predecessor A splits into four edges, D, C, B and F, and produces a marker E (Figure 1a). Successor edges D and B have the same direction as A, edge C has the opposite direction, and F is neutral. Marker E is placed to the right of A and is directed towards A. As an example of a production with a neutral predecessor, consider $\mathtt{A} \rightarrow \vec{\mathtt{B}}[-\overleftarrow{\mathtt{B}}]\mathtt{x}[+\overleftarrow{\mathtt{B}}]\overleftarrow{\mathtt{B}}$. In this case the result of production application does not depend on the assumed direction of the predecessor edge (Figure 1b).

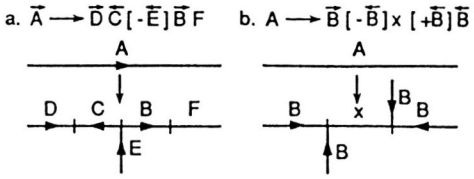

Figure 1: Examples of edge productions.

A *derivation step* in an mBPM0L-system consists of two phases.

1. Each edge in the map is replaced by successor edges and markers using the corresponding edge production in P.
2. Each region is scanned for *matching markers*. If a match is found, the markers are joined to create a new edge which will split the region.

Two markers are considered matching if:

1. they appear in the same region,
2. they have the same label, and
3. one marker is directed away from its incident edge while the other is directed towards the edge, or both markers are neutral.

The search for matching markers ends with the first match found, even though other markers entering the same region may also form a match. From the user's perspective, the system behaves in a nondeterministic way, since it autonomously chooses the pair of markers to be connected. The unused markers are discarded.

We will illustrate the operation of mBPM0L-systems using two examples.

```
L-system 1

ω :  ABAB
p1 :  A  →  B[−A][+A]B
p2 :  B  →  A
```

In L-system 1, production p_1 creates markers responsible for region division while production p_2 introduces a delay. As a result the regions are subdivided alternately by horizontal and vertical edges (Figure 2).

L-system 2 illustrates the operation of an mBPM0L-system with directed edges. Productions p_1 and p_3 create markers. Production p_4 transforms edge D into C, so that in each derivation step there is a pair of edges A and C to which productions p_1 and p_3 apply. Production p_2 indicates that edges B do not undergo further

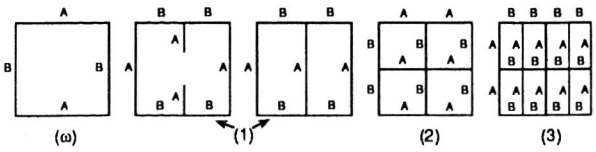

Figure 2: Developmental sequence defined by L-system 1. In the first step, a distinction is made between the edge-rewriting phase and the connection of matching markers.

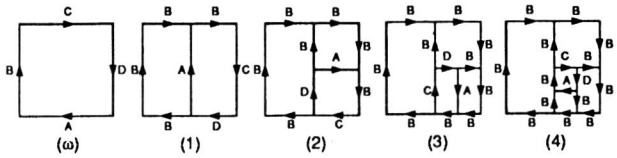

Figure 3: Developmental sequence defined by L-system 2.

L-system 2

ω : $\vec{A}\,\vec{B}\,\vec{C}\,\vec{D}$

p_1 : $\vec{A} \rightarrow \vec{D}\,[-\,\vec{A}\,]\,\vec{B}$

p_2 : $\vec{B} \rightarrow \vec{B}$

p_3 : $\vec{C} \rightarrow \vec{B}\,[-\,\vec{A}\,]\,\vec{B}$

p_4 : $\vec{D} \rightarrow \vec{C}$

changes.[2] The resulting structure is that of a clockwise spiral (Figure 3).

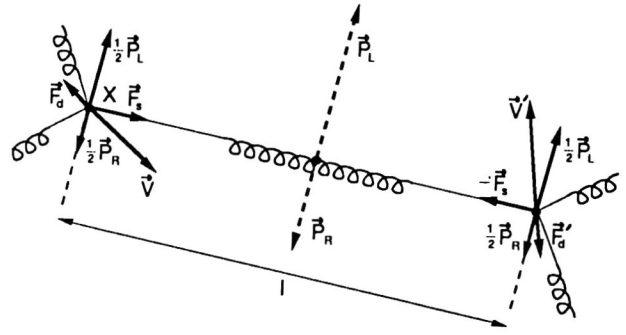

Figure 4: Forces acting on a cell corner X according to the dynamic method.

2.3 Dynamic Interpretation

Maps are topological objects without inherent geometric properties. In order to visualize them, some method for assigning geometric interpretation must be applied. We describe it using biologically-motivated terms, cell and wall, instead of their mathematical counterparts, region and edge.

Assuming the dynamic point of view, the shape of cells and thus the shape of the entire organism result from the action of forces. The unbalanced forces due to cell divisions cause the gradual modification of cell shapes until an equilibrium is reached. At this point, new cell divisions occur, and expansion resumes.

The dynamic method for determining cell geometry is based on the following assumptions:

- the modeled organism forms a single cell layer,
- the layer is represented as a two-dimensional network of masses corresponding to cell corners, connected by springs which correspond to cell walls,
- the springs are always straight and adhere to Hooke's law,
- the cells exert pressure on their bounding walls; the pressure on a wall is directly proportional to the wall length and inversely proportional to the cell area,
- the pressure on a wall spreads evenly between the wall corners,
- the motion of masses is damped, and
- no other forces are considered.

The position of each vertex, and thus the shape of the cell layer, is computed as follows. As long as an equilibrium is not reached, unbalanced forces put masses in motion. The total force $\vec{F}_T$ acting on a vertex X is given by the formula:

$$\vec{F}_T = \sum_{w \in W} \vec{F}_w + \vec{F}_d$$

where:

- $\vec{F}_w$ are forces contributed by the set of walls W incident to X, and
- $\vec{F}_d = -b\vec{v}$ is a damping force, expressed as the product of a damping factor b and vertex velocity $\vec{v}$.

A wall $w \in W$ contributes three forces acting on X (Figure 4). The *tension* $\vec{F}_s$ acts along the wall and its magnitude is determined by Hooke's law, $F_s = -k(l - l_0)$, where k is the spring constant, l is the current spring length, and l_0 is the rest length. The remaining two forces, $\vec{P}_L$ and $\vec{P}_R$, are due to the *pressure* exerted by the cells on the left side and on the right side of the wall. Each force acts in the direction perpendicular to the wall, and is distributed equally between its two incident vertices. The magnitude of the force $\vec{P}_L$ exerted by the

[2] In further L-systems such identity productions are omitted.

cell on the left side of the wall equals $p_L \cdot l$, where p_L is the internal cell pressure and l is the wall length. A similar formula describes the force $\vec{P}_R$. The pressure is assumed to be inversely proportional to the cell area: $p \sim A^{-1}$. This assumption is derived from the equation describing osmotic pressure, $p = SRT$, as a function of the concentration of the solute S (n moles per volume V of the solution), the ideal gas constant R, and the absolute temperature T [11]. Assuming that the cell volume V is proportional to the area A captured by the two-dimensional model under consideration ($V = Ah$), pressure can be expressed as

$$p = \frac{nRT}{Ah}.$$

Thus, $p \sim A^{-1}$, provided that the term nRT/h is constant.

A convenient formula for calculating the area A is:

$$A = |\sum_{i=1}^{M} (x_i - x_{i+1})(y_i + y_{i+1})/2|$$

where (x_i, y_i) are coordinates of the M vertices surrounding region A, $x_{M+1} = x_1$, and $y_{M+1} = y_1$ [2].

The force $\vec{F}_T$ acts on a mass placed at a map vertex. Newton's second law of motion applies:

$$m\frac{d^2\vec{x}}{dt^2} = \vec{F}_T$$

where $\vec{x}$ is the vertex position. If the entire structure has N vertices, we obtain a system of $2N$ differential equations:

$$\begin{aligned} m_i\frac{d\vec{v}_i}{dt} &= \vec{F}_{T_i}(\vec{x}_1, \cdots, \vec{x}_N, \vec{v}_i) \\ \frac{d\vec{x}_i}{dt} &= \vec{v}_i \end{aligned}$$

where $i = 1, 2, \ldots, N$. The task is to find the sequence of positions $\vec{x}_1, \ldots, \vec{x}_N$ at given time intervals, assuming that the functions $\vec{F}_{T_i}$ and the initial values of all variables: $\vec{x}_1^0, \ldots, \vec{x}_N^0$ and $\vec{v}_1^0, \ldots, \vec{v}_N^0$ are known. These initial values are determined as follows:

- Coordinates of the vertices of the starting map are included in the input data for the simulation.
- Positions of existing vertices are preserved through a derivation step. New vertices partition the divided walls into segments of equal length. The initial velocities of all vertices are set to zero.

The system of differential equations with the initial values given above represents an *initial value problem*. It can be solved numerically using the *forward (explicit) Euler method* [4]. To this end, the differential equations are rewritten using finite increments $\Delta\vec{v}_i$, $\Delta\vec{x}_i$ and Δt:

$$\begin{aligned} \Delta\vec{v}_i^{\,k} &= \frac{1}{m_i}\vec{F}_{T_i}\left(\vec{x}_1^{\,k}, \cdots, \vec{x}_N^{\,k}, \vec{v}_i^{\,k}\right)\Delta t \\ \Delta\vec{x}_i^{\,k} &= \vec{v}_i^{\,k}\Delta t \end{aligned}$$

where the superscripts $k = 0, 1, 2, \ldots$ indicate the progress of time, $t = k\Delta t$. The position and velocity of a point i after time increment Δt are expressed as follows:

$$\begin{aligned} \vec{v}_i^{\,k+1} &= \vec{v}_i^{\,k} + \Delta\vec{v}_i^{\,k} \\ \vec{x}_i^{\,k+1} &= \vec{x}_i^{\,k} + \Delta\vec{v}_x^{\,k} \end{aligned}$$

The iterative computation of the velocities $\vec{v}_i^{\,k}$ and positions $\vec{x}_i^{\,k}$ is carried out for consecutive values of index k until all increments $\Delta\vec{v}_i$ and $\Delta\vec{x}_i$ fall below a threshold value. This indicates that the equilibrium state has been approximated to the desired accuracy. The next derivation step is then performed. A system of equations corresponding to the new map topology is created, and the search for an equilibrium state resumes. In such a way, the developmental process is simulated as periods of continuous cell expansion, delimited by instantaneous cell divisions. Continuity of cell shapes during divisions is preserved by the rule which sets the initial positions of vertices.

2.4 Biological Examples

In this section, the described simulation method is applied to visualize the development of two fern gametophytes *Microsorium linguaeforme* and *Dryopteris thelypteris*, and a moss leaf *Phascum cuspidatum*. All of these structures form single cell layers. Their development can be described conveniently in terms of two types of activities: the activity of the *apical cell* giving rise to cell clones called *segments*, produced alternately to the left and to the right of the apex, and the development of these segments. The construction of map L-systems based on microscopic observations is a nontrivial task, requiring a good understanding of the underlying biological processes. This problem is discussed further in [3, 5].

2.4.1 Microsorium linguaeforme

Map L-system 3, explained in [3, 5], captures the development of a fern gametophyte *Microsorium linguaeforme*. The essential part of the starting map (without basal segments) is shown in Figure 5(0). Productions describing the development of the right side of the organism are given explicitly. Their predecessors are denoted by uppercase letters. The corresponding lowercase productions, which complete the L-system definition, can be obtained by switching the "case" of letters and the orientation of markers while leaving the wall directions unchanged. For example, the right-side production $r_1 : \vec{A} \rightarrow \overleftarrow{a}\,[-\,\overleftarrow{B}]\,\vec{I}$ corresponds to the left-side production, $l_1 : \vec{a} \rightarrow \overleftarrow{A}\,[+\,\overleftarrow{b}]\,\vec{i}$.

The L-system operation is illustrated in Figure 5. The

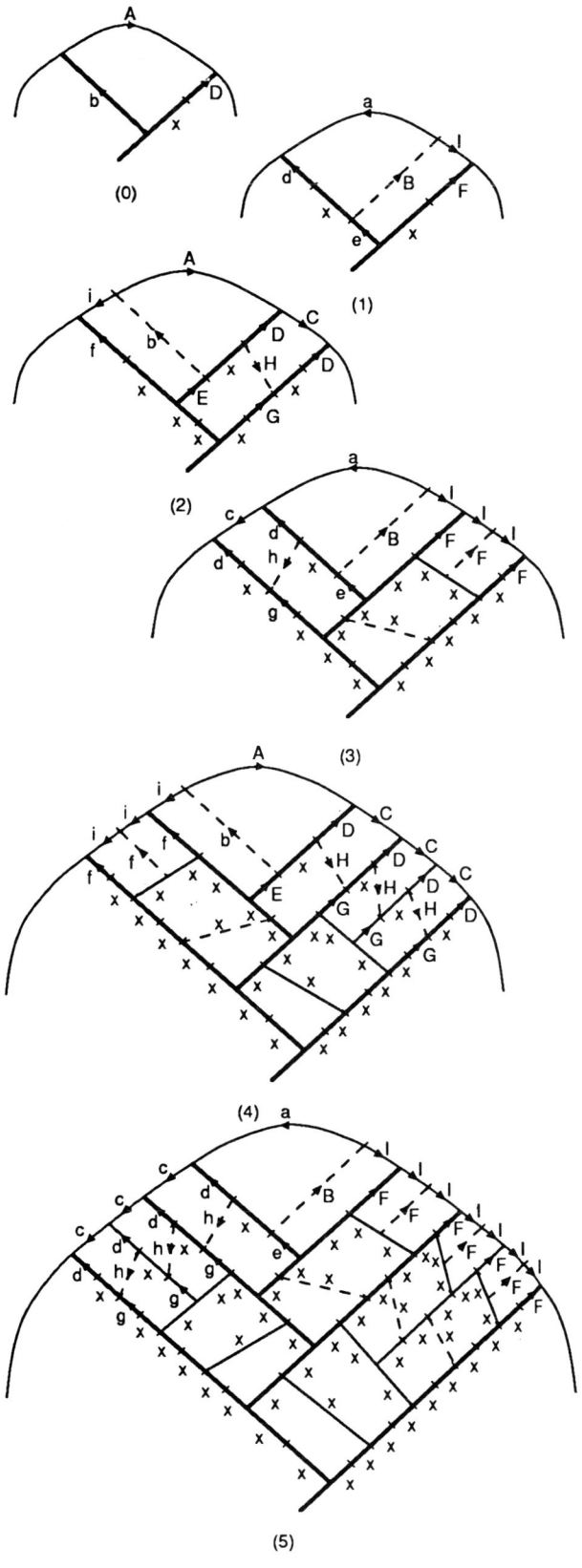

Figure 5: A diagrammatic representation of the developmental sequence of a *Microsorium* gametophyte.

L-system 3: Microsorium

$$
\begin{aligned}
r_1 &: \overrightarrow{A} \rightarrow \overleftarrow{a}\,[-\,\overleftarrow{B}]\,\overrightarrow{I}\\
r_2 &: \overrightarrow{B} \rightarrow \overrightarrow{E}\,[+\,\overrightarrow{b}]\,x\,[-\,\overrightarrow{H}]\,\overrightarrow{D}\\
r_3 &: \overrightarrow{D} \rightarrow [-\,\overrightarrow{m}]\,\overrightarrow{F}\\
r_4 &: \overrightarrow{F} \rightarrow \overrightarrow{G}\,[+\,\overleftarrow{H}]\,x\,[-\,\overrightarrow{H}]\,\overrightarrow{D}\\
r_5 &: \overrightarrow{H} \rightarrow x\,[+\,\overrightarrow{F}]\,x\\
r_6 &: \overrightarrow{I} \rightarrow \overrightarrow{C}\\
r_7 &: \overrightarrow{C} \rightarrow \overrightarrow{I}\,[-\,\overleftarrow{F}]\,\overrightarrow{I}\\
r_8 &: \overrightarrow{E} \rightarrow x\,[-\,x]\,x\\
r_9 &: \overrightarrow{G} \rightarrow x\,[+\,x]\,x\,[-\,x]\,x\\
r_{10} &: \overrightarrow{J} \rightarrow \overrightarrow{L}\\
r_{11} &: \overrightarrow{K} \rightarrow \overrightarrow{N}\\
r_{12} &: \overrightarrow{L} \rightarrow x\,[-\,\overleftarrow{M}]\,x\\
r_{13} &: \overrightarrow{M} \rightarrow x\,[-\,\overrightarrow{L}]\,x\\
r_{14} &: \overrightarrow{N} \rightarrow \overrightarrow{O}\\
r_{15} &: \overrightarrow{O} \rightarrow x\,[-\,\overleftarrow{L}]\,\overrightarrow{N}
\end{aligned}
$$

apical cell divisions result from the application of productions r_1 and r_2 as well as their symmetric counterparts, l_1 and l_2. The segment cell divisions proceed symmetrically in right and left segments according to productions $r_3 - r_9$ and $l_3 - l_9$. The development of basal segments is controlled by productions $r_{10} - r_{15}$ and $l_{10} - l_{15}$.

A simulated developmental sequence generated by L-system 3 using the dynamic method to determine cell shapes is given in Plate 1. Different colors are used to indicate the apical cell, the alternating "regular" segments, and the basal segments. A comparison with a microphotograph of *Microsorium linguaeforme* (Plate 2) shows good correspondence between the model and reality with respect to structure topology, the relative sizes and shapes of cells, and the overall shape of the organism.

2.4.2 Further Examples

Gametophytes of other fern species follow a similar developmental pattern, with the apex producing segments alternately to the left and to the right. However, the cell division patterns within segments vary between species, yielding different overall shapes. For example, Plate 3 shows the development of the heart-shaped gametophyte *Dryopteris thelypteris*. The map L-system is given in [3].

Nägeli [9] studied the moss *Phascum cuspidatum* and proposed a scheme for the apical development of its leaves, similar to that of fern gametophytes. A simulated developmental sequence based on Nägeli's observations is shown in Plate 4.

3 Modeling Spherical Cell Layers

During the *cleavage* stage of development, an embryo consists of a single layer of cells which covers the surface of a spherical cavity. This structure is known as the *blastula* [1]. The cells divide synchronously in a regular pattern up to and including the 64-cell stage (6th cleavage). This development can be captured using an mBPM0L-system operating on the surface of a sphere rather than on a plane. To this end, cell walls are represented as great circle arcs connecting vertices which are constrained to the sphere surface.

The extension of the dynamic interpretation method from the plane to the surface of a sphere requires few changes. Osmotic pressure and wall tension are calculated as before. Since the resulting force may displace a vertex away from the surface of the sphere, the actual vertex position is found by projecting the displaced point back to the sphere. Cells of embryos at the cleavage stage do not expand, thus the overall size of the sphere is constant.

For example, map L-system 4 was proposed in [3] to model the development of a snail embryo *Patella vulgata* according to data presented in [13]. The starting map and developmental sequence are shown in Figure 6. Plate 5 presents an alternative rendering of the modeled structures. Each cell is approximated by a sphere centered at the point representing the center of gravity of the cell corners and raised to the surface of the underlying spherical cavity. The radius is the maximum distance from the center to the cell corners. A comparison to an electron microscope image (Plate 6) of the equatorial view of *Patella* at the 16-cell stage shows good correspondence between the model and reality.

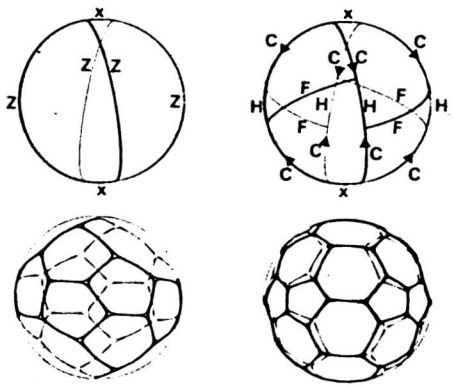

Figure 6: Developmental sequence of *Patella vulgata* (equatorial view).

L-system 4: Patella

p_1 : A → b[−a]x[+a]b
p_2 : a → B[+A]x[−A]B
p_3 : B → a
p_4 : b → A
p_5 : $\overrightarrow{C}$ → $\overrightarrow{D}$ [+a] $\overrightarrow{E}$
p_6 : $\overrightarrow{D}$ → $\overrightarrow{C}$ [−A]x
p_7 : $\overrightarrow{E}$ → $\overrightarrow{C}$
p_8 : F → $\overleftarrow{E}$ [−a]G[+a] $\overrightarrow{E}$
p_9 : G → J
p_{10} : H → I
p_{11} : I → B[−A]x[+A]B
p_{12} : J → b[+a]x[−a]b
p_{13} : Z → $\overrightarrow{C}$ [−F]H[+F] $\overleftarrow{C}$

4 Modeling 3D Cellular Structures

4.1 Cellworks

In [7], Lindenmayer proposed *cellworks* to represent 3D multicellular structures. They extend the notion of maps to three dimensions as follows:

- A cellwork is a finite set of *cells*. Each cell is surrounded by one or more *walls* (faces).
- Each wall is surrounded by a boundary consisting of a finite, circular sequence of *edges* which meet at *vertices*.
- Walls cannot intersect without forming an edge, although there can be walls without edges.[3]
- Every wall is part of the boundary of a cell, and the set of walls is connected.
- Each edge has one or two vertices associated with it. The edges cannot cross without forming a vertex and there are no vertices without an associated edge.
- Every edge is a part of the boundary of a wall and the set of edges is connected.

Note that the terms *cell* and *wall* have different meanings in the contexts of cellworks and maps.

[3] In the case of cells shaped as spheres or toruses.

4.2 mBPC0L-systems

In order to model development of three-dimensional structures, we propose an extension of mBPM0L-systems called *marker Binary Propagating Cellwork 0L-systems*. An mBPC0L-system $\mathcal{G}$ is defined by a finite alphabet of *edge labels* Σ, a finite alphabet of *wall labels* Γ, a *starting cellwork* ω and a finite set of *edge productions* P. The initial cellwork ω is specified by a list of walls and their bounding edges. As in the case of mBPM0L-systems, edges may be directed or neutral. Each production is of the form $\mathtt{A} : \beta \rightarrow \alpha$, where the edge $\mathtt{A} \in \Sigma$ is the *predecessor*, the string $\beta \in \{\Gamma^+, *\}$ is a list of *applicable walls* (* denotes all walls), and the string α, composed of edge labels from Σ, wall labels

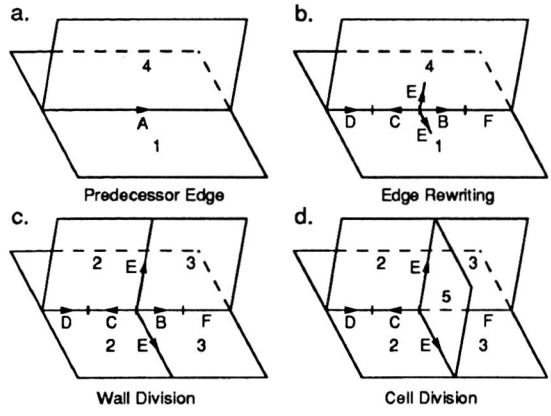

Figure 7: The phases of a derivation step.

from Γ and symbols [and], is the *successor*. The sequence of symbols outside the square brackets describes the subdivision pattern for the predecessor. Pairs of matching brackets [and] delimit *markers* which specify possible attachment sites for new edges and walls. As in the 2D case, arrows indicate the directions of the successor edges and markers with respect to the predecessor edge. The list β contains all walls into which a marker should be inserted. In addition to the labels for edges and markers, a production successor specifies the labels of walls which may be created as a result of a derivation step.

The syntax of a production is best explained using an example. Production $\vec{\mathtt{A}}: 14 \rightarrow \vec{\mathtt{D}}\,\overleftarrow{\mathtt{C}}_2[\vec{\mathtt{E}}_5]\vec{\mathtt{B}}_3\,\mathtt{F}$ applies to the edge A if it belongs to one or more walls labeled 1 or 4 (Figure 7a). The predecessor edge is subdivided into four edges D, C, B and F. Marker E is introduced into all walls of type 1 or 4 which share edge A (Figure 7b). During a derivation step, marker E may be connected with a matching marker inserted into the same wall by another production. As a result, the wall will split into two. The daughter wall having C as one of its edges will be labeled 2, and the wall having B as an edge will be labeled 3 (Figure 7c). The Markers E will be connected only if both productions label the daughter walls in a consistent way. Otherwise, the markers are considered non-matching and are discarded. If several walls, bounding a cell, split in such a way that the sequence of new edges forms a closed contour, a new wall, bound by these edges, may be created. In order for this to happen, all markers involved must specify the same label for the new wall, 5 in this example (Figure 7d).

The limitation of a production's scope to specific walls may create a consistency problem while rewriting edges. For instance, assume that walls 1 and 2 share edge A, and the following productions are in P:

$$\begin{aligned} p_1: &\quad \vec{\mathtt{A}}:1 \rightarrow \vec{\mathtt{C}}\,\overleftarrow{\mathtt{E}} \\ p_2: &\quad \vec{\mathtt{A}}:2 \rightarrow \mathtt{A}\,\vec{\mathtt{B}} \end{aligned}$$

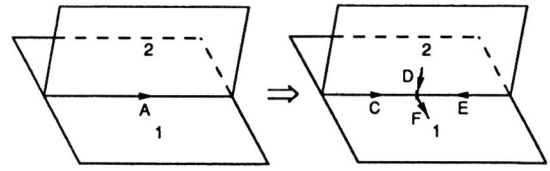

Figure 8: Example of consistent edge productions.

Productions p_1 and p_2 are inconsistent since they specify two different partitions of the same edge. We assume that the mBPC0L-systems under consideration are free of such inconsistencies. This does not preclude the possibility of applying several productions simultaneously to the same edge. For example, a production pair,

$$\begin{aligned} p_1: &\quad \vec{\mathtt{A}}:1 \rightarrow \vec{\mathtt{C}}_2[\vec{\mathtt{F}}_3]\overleftarrow{\mathtt{E}}_4 \\ p_2: &\quad \vec{\mathtt{A}}:2 \rightarrow \vec{\mathtt{C}}_5[\overleftarrow{\mathtt{D}}_6]\overleftarrow{\mathtt{E}}_7 \end{aligned}$$

consistently divides edge A into segments C and E, although the markers inserted into walls 1 and 2 are different (Figure 8).

According to the above discussion, a *derivation step* in an mBPC0L-system consists of three phases:

1. Each edge in the cellwork is replaced by successor edges and markers using one or more productions in P.
2. Each wall is scanned for matching markers. If a match inducing a consistent labeling of daughter cells is found, the wall is subdivided. The selection of matching markers is done by the system. The unused markers are discarded.
3. Each cell is scanned for a circular sequence of new division edges. If a cycle assigning the same label to the division wall is found, it is used to bound the wall which will divide the cell into two daughter cells. If different possibilities exist, the edges are selected by the system.

A wall may be subdivided more than once as long as new division edges do not intersect and a consistent labeling of daughter walls is possible. In contrast, a cell may be divided only once in any derivation step.

For example, consider the following three-dimensional extension of L-system 1.

L-system 5

$$\begin{aligned} p_1: &\quad \mathtt{A}:1 \rightarrow \mathtt{B}_1[\mathtt{A}_2]\mathtt{B}_1 \\ p_2: &\quad \mathtt{A}:2 \rightarrow \mathtt{B}_2[\mathtt{C}_2]\mathtt{B}_2 \\ p_3: &\quad \mathtt{B}:* \rightarrow \mathtt{A} \end{aligned}$$

The starting cellwork ω and the resulting developmental sequence of cellworks are shown in Figure 9. In the first

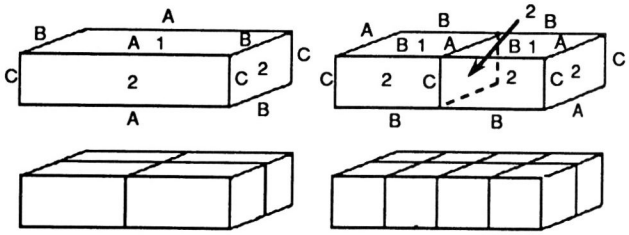

Figure 9: Developmental sequence generated by L-system 7.

derivation step, production p_1 divides walls labeled 1, and production p_2 divides walls labeled 2. The new division edges form a cycle which divides the cell with a new wall labeled 2. In the subsequent steps this process is repeated, generating a pattern of alternating division walls. Production p_3 introduces the necessary delay.

4.3 Dynamic Interpretation of mBPC0L-systems

The dynamic method for interpreting map L-systems is extended to cellwork L-systems using the following assumptions:

- the modeled organism forms a 3-dimensional multicellular structure,
- the structure is represented as a three-dimensional network of masses corresponding to cell corners, connected by springs which correspond to cell edges,
- the springs are always straight and adhere to Hooke's law,
- for the purpose of force calculations, walls can be approximated by flat polygons,
- the cells exert pressure on their bounding walls; the pressure on a wall is directly proportional to the wall area and inversely proportional to the cell volume,
- the pressure on a wall spreads evenly between the wall corners,
- the motion of masses is damped, and
- other forces are not considered.

The position of each vertex is computed as follows. The total force $\vec{F}_T$ acting on a vertex X is given by the formula:

$$\vec{F}_T = \sum_{e \in E} \vec{F}_e + \sum_{w \in W} \vec{F}_w + \vec{F}_d,$$

where:

- $\vec{F}_e$ are forces contributed by the set of edges E incident to X,
- $\vec{F}_w$ are forces contributed by the set of walls W incident to X, and
- $\vec{F}_d = -b\vec{v}$ is a damping force.

The forces $\vec{F}_e$ act along the cell edges and represent wall *tension*. They follow Hooke's law, as in the two-dimensional case. The forces $\vec{F}_w$ are due to the *pressure* exerted by the cells on their bounding walls. The total force of pressure $\vec{P}$ exerted by a cell on a wall w has direction normal to w and is equal to $p \cdot A$, where p is the internal cell pressure and A is the wall area. Calculation of the polygon area proceeds as in two-dimensional case. The pressure p is assumed to be inversely proportional to the cell volume, $p \sim V^{-1}$, which corresponds to the equation describing osmotic pressure. The volume V of a cell is calculated by tesselating the cell into tetrahedra. The resulting differential equations are formed and solved as in the 2D case.

4.4 Development of Epidermal Cells

The mBPC0L-system 6 describes a division pattern which frequently occurs in epidermal cell structures. It is based on a cyclic cellwork L-system (a slightly different formalism) presented in [7].

L-system 6

p_1 : A : 123 → $C_3[E_1]B_2[D_1]C_3$
p_2 : A : 4 → $CB_4[F_1]C_4$
p_3 : B : * → A
p_4 : C : * → B
p_5 : E : * → D
p_6 : F : 123 → HGH
p_7 : F : 4 → $H_4[F_1]G_4[F_1]H_4$
p_8 : G : * → F
p_9 : H : * → G

The starting cellwork and a simulated developmental sequence generated by L-system 6 using the dynamic method to determine cell shapes are shown in Figure 10. Productions p_1, p_2, p_6, and p_7 are responsible for edge, wall and cell divisions, while the remaining productions introduce delays such that the division pattern is staggered.

5 Conclusions

This paper presented a modeling method for three classes of multicellular structures: planar cell layers, cell layers on a sphere, and three-dimensional cellular structures. In the first two cases, the topology is captured using mBPM0L-systems. The 3D case relies on an extension of map L-systems, called mBPC0L-systems. In all cases, the geometry results from a dynamic model that takes into account internal cell pressure and wall

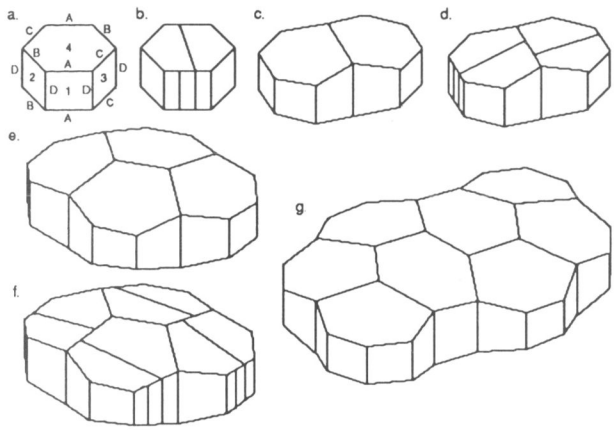

Figure 10: Developmental sequence of epidermal cells. (a) The starting cellwork. (b,d,f) Cellworks immediately after cell divisions. (c,e,g) The corresponding cellworks at equilibrium.

tension. The method is illustrated using a number of biological models which show good correspondence with their natural counterparts.

The dynamic method for determining cell shapes involves many arbitrary assumptions, such as equal distribution of pressure between the wall vertices, and reduction of wall tension to forces acting along the wall edges. It is tempting to introduce more sophisticated assumptions concerning physical properties of cells and their components. At this time we are not aware of biological observations which would provide a solid basis for such refinements.

The lack of data presents an obstacle to the modeling of three-dimensional structures using mBPC0L-systems. For example, we attempted to model the development of a root of *Azolla pinnata*, presented in [6] and frequently quoted in biological literature, but the available description was too general to be captured in the form of an mBPC0L-system.

Acknowledgements

We are deeply indebted to Professor Lindenmayer for inspiring discussions and comments on earlier versions of this paper. Norma Fuller contributed routines supporting geometric operations on a sphere. The reported research has been supported by an operating grant, equipment grants and a scholarship from the Natural Sciences and Engineering Research Council of Canada. Facilities of the Department of Computer Science, University of Regina, were also essential. All support is gratefully acknowledged. Thanks also to the reviewers for their helpful comments and suggestions.

References

[1] B. I. Balinsky. *An introduction to embryology.* W. B. Saunders Co., Philadelphia, 3rd edition, 1970.

[2] S. Bronshtein. *Handbook of mathematics.* Van Nostrand, New York, 1985.

[3] M. J. M. de Boer. *Analysis and computer generation of division patterns in cell layers using developmental algorithms.* PhD thesis, University of Utrecht, the Netherlands, 1989.

[4] L. Fox and D. F. Mayers. *Numerical solution of ordinary differential equations.* Chapman and Hall, London, 1987.

[5] F. D. Fracchia, P. Prusinkiewicz, and M. J. M. de Boer. Animation of the development of multicellular structures. To appear in, D. Thalmann, editor, *Computer Animation '90,* Springer-Verlag, 1990.

[6] B. E. S. Gunning. Microtubules and cytomorphogenesis in a developing organ: the root primordium of Azolla pinnata. In O. Kiermayer, editor, *Cytomorphogenesis in plants,* pages 301–325. Springer-Verlag, Wien, 1981. Cell biology monographs 8.

[7] A. Lindenmayer. Models for plant tissue development with cell division orientation regulated by preprophase bands of microtubules. *Differentiation,* 26:1–10, 1984.

[8] A. Lindenmayer and G. Rozenberg. Parallel generation of maps: developmental systems for cell layers. In V. Claus, H. Ehrig, and G. Rozenberg, editors, *Graph-grammars and their application to computer science and biology,* pages 301–316. Springer-Verlag, Berlin, 1979. Lecture Notes in Comp. Sci. 73.

[9] C. Nägeli. Wachsthumsgeschichte der Laub- und Lebermoose. *Zeitschr für Wissensch, Botanik,* 2:138–210, 1845.

[10] A. Nakamura, A. Lindenmayer, and K. Aizawa. Some systems for map generation. In G. Rozenberg and A. Salomaa, editors, *The Book of L,* pages 323–332. Springer-Verlag, Berlin, 1986.

[11] F. W. Sears, M. W. Zemansky, and H. D. Young. *College physics.* Addison-Wesley Publ. Co., Reading, 6th edition, 1985.

[12] W. T. Tutte. *Graph theory.* Addison-Wesley Publ. Co., Reading, 1982.

[13] J. A. M. van den Biggelaar. Development of dorsoventral polarity and mesentoblast determination in Patella vulgata. *Journal of Morphology,* 154:157–186, 1977.

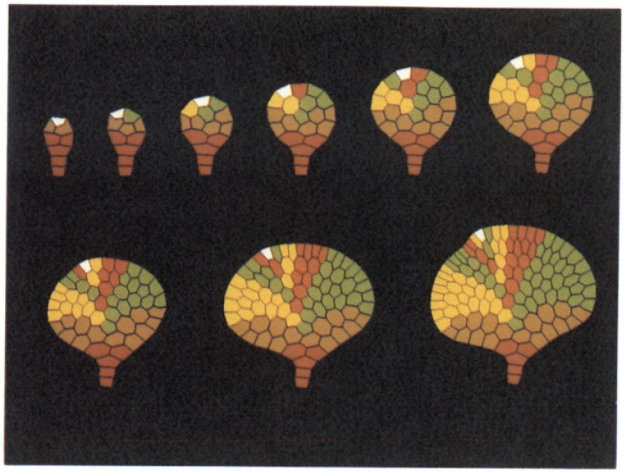

Plate 1: Simulated developmental sequence of *Microsorium linguaeforme.*

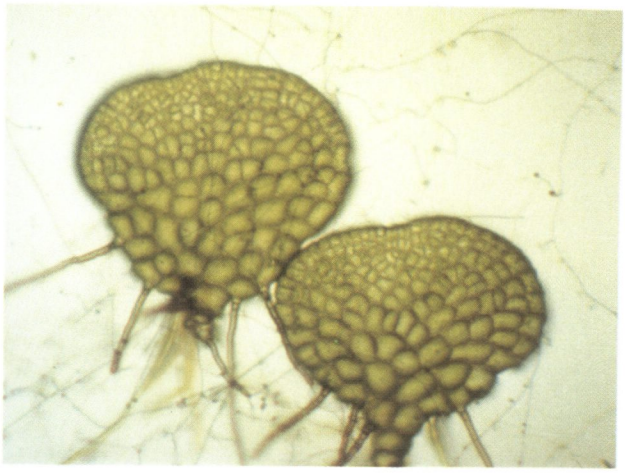

Plate 2: Microphotograph of *Microsorium linguaeforme* at magnification 70x.

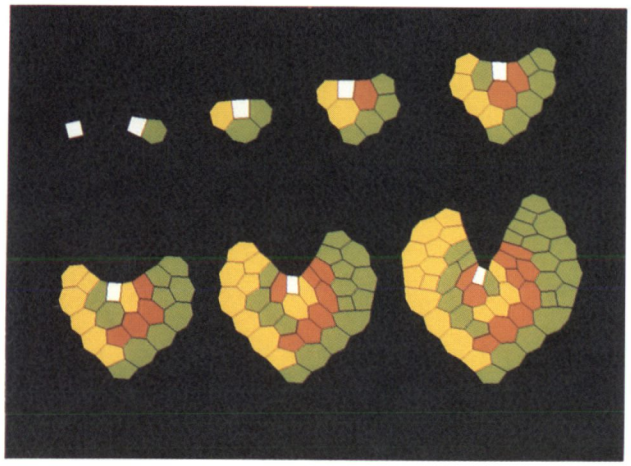

Plate 3: Simulated developmental sequence of *Dryopteris thelypteris.*

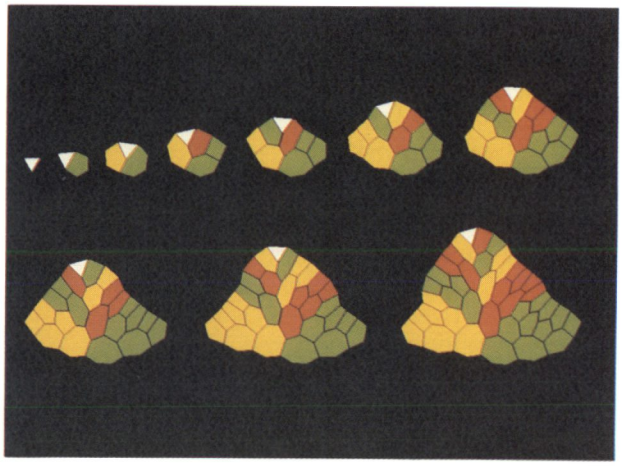

Plate 4: Simulated developmental sequence of *Phascum cuspidatum.*

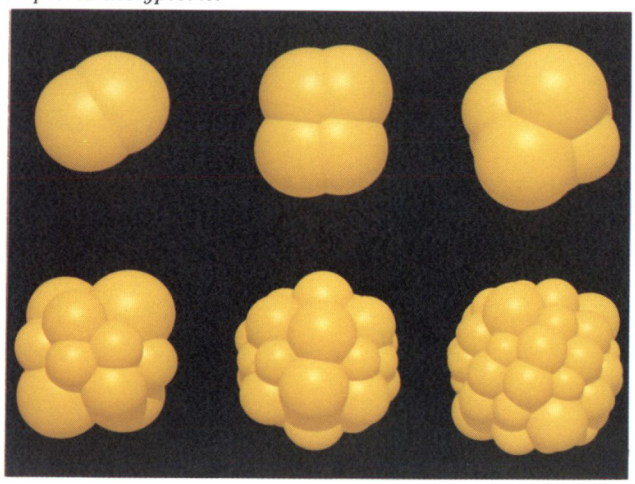

Plate 5: Simulated developmental sequence of *Patella vulgata.*

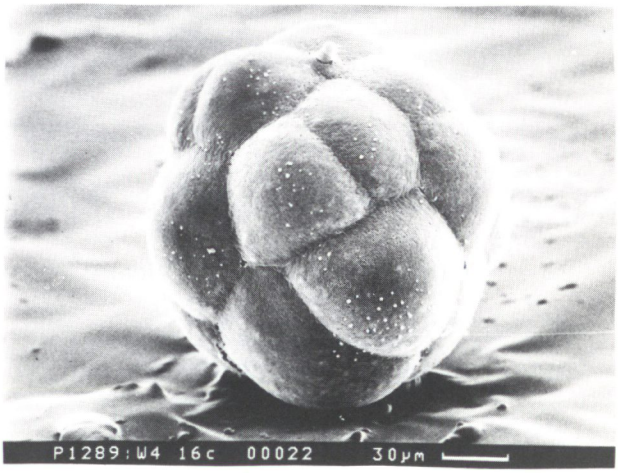

Plate 6: Electron microphotograph of *Patella vulgata* (courtesy of Willem J. A. G. Dictus, University of Utrecht).